Frequency and temperature dependent dielectric and conductivity behavior of KNbO$_3$ ceramics

B. Sundarakannan,[a] K. Kakimoto, and H. Ohsato
Department of Material Science and Engineering, Nagoya Institute of Technology, Showa-ku, Nagoya-466 8555, Japan

Dielectric and conductivity measurements were carried out on the potassium niobate ceramics both as a function of temperature (50 to 550 °C) and frequency (10^2 to 10^6 Hz). A low-frequency dielectric relaxation in the temperature range of 100 to 200 °C is observed and analyzed with the Cole–Cole function. The activation energy of dielectric relaxation is estimated to be 0.84 eV. Frequency dependent conductivity data are analyzed with an augmented Jonscher relation. Potassium niobate exhibits universal conductivity behavior. Activation energies obtained for the dc conductivity and the hopping frequency are 1.01 and 0.94 eV, respectively. A possible mechanism for both the low-frequency dielectric relaxation and the frequency dependent conductivity is proposed based on activation energies and off stoichiometry of KNbO$_3$, which is resulted due to potassium oxide evaporation during preparation processes. © *2003 American Institute of Physics.*
[DOI: 10.1063/1.1610260]

I. INTRODUCTION

Potassium niobate, KNbO$_3$ (KN), single crystals have been thoroughly studied due to their applications in nonlinear optical, surface acoustic wave (SAW), and electromechanical transducer devices (for example, see Ref. 1). Ferroelectric KNbO$_3$ exhibits three successive phase transitions similar to that of BaTiO$_3$.[2] Despite well documented data and an understanding of the dielectric behavior of the KN single crystals, work on polycrystalline/ceramic materials is scanty due to the inherent difficulties related to the sintering process. Recently, potassium niobate ceramics were revisited in the interest of a search for environmental friendly lead-free piezoelectric materials.[3] Hence, the work on the potassium niobate ceramics gained importance.

A dielectric investigation on KNbO$_3$ ceramics sintered with LiF additive was reported by Dubernet and Ravez[4] over a wide frequency (10^2 to 10^9 Hz) and temperature (300 to 800 K) range. Their report deals with a detailed study on a high-frequency ($\sim 10^8$ Hz) dielectric relaxation originating due to network relaxations at temperatures just below and above the Curie temperature (670 K) and also indicates a frequency dependence of the permittivity due to conductivity at temperatures above 500 K.[4] A frequency dependent contribution to the dielectric constant of LiTaO$_3$ single crystals was attributed to the mobile charged point defects connected with the nonstoichiometry of the crystal.[5]

The frequency dependent conductivity of KNb$_x$V$_{1-x}$O$_3$ ($x=0,0.1$) single crystals measured below the temperatures of 430 °C was reported.[6] Specifically, a marked difference in the behavior of frequency (10 to 10^6 Hz) dependent conductivity above and below 250 °C data was shown for undoped KN single crystals. They reported that the power-law exponent of the conductivity varies from 1 to 0.7 when the tem-

perature varies from 30 to 430 °C for pure potassium niobate and activation energy of the dc conductivity is 1.02 eV.[6]

The present article describes dielectric and conductivity investigations both as a function of temperature and frequency carried out on potassium niobate ceramics using an impedance analyzer. A low-frequency dielectric relaxation and frequency dependent conductivity are observed from the aforementioned measurements. The respective data were analyzed by the semiempirical complex Cole–Cole equation and the augmented Jonscher relation. The results are discussed in light of inadvertent potassium oxide evaporation induced off-stoichiometric vacancy defects present in the potassium niobate ceramics.

II. EXPERIMENT

Potassium niobate ceramics were prepared by following the conventional ceramic method. An equimolar ratio of K$_2$CO$_3$ (99.9%) and Nb$_2$O$_5$ (99.9%) was milled in an acetone medium with zirconia balls for 24 h. The dried powder mixture was calcined at 830 °C three times with an intermediate hand grinding to ensure the completion of the reaction.[7] Binder (polyvinyl alcohol 5 wt %) mixed powder was shaped to a disk form at a pressure of 15 MPa in uniaxial pressing. To improve the sinterability, two additional measures were adopted. They are sintering at temperatures close to the melting point and sintering the pellets within a powder matrix. Sintering was carried out at 1020 °C for 2 h in air with a KN powder matrix. The measured relative density of pellet is above 95%. Gold electrodes were coated on both the sides of the pellet, which is 10 mm in diameter and 1 mm in thickness.

The phase characterization of the ceramics was done on the x-ray diffraction (XRD) patterns recorded using an x-ray diffractometer (Philips X'Pert MPD, Kanagawa, Japan). The capacitance, tangent loss, and conductance were measured

---

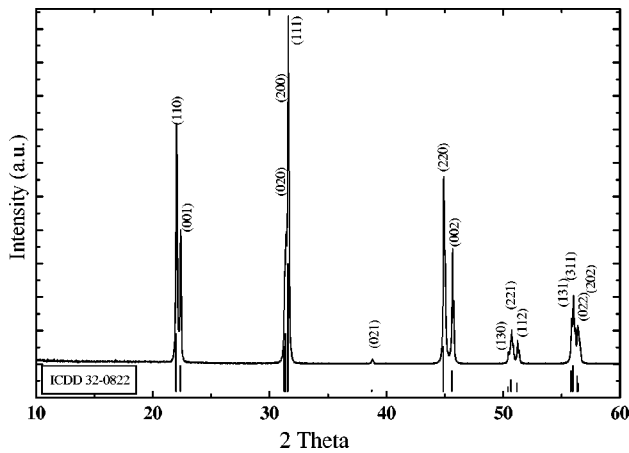[a]Electronic mail: suka@zymail.mse.nitech.ac.jp

FIG. 1. Powder XRD pattern of potassium niobate. The vertical lines in the bottom are ICDD data.

using a impedance analyzer (Agilent 4294A, Kobe, Japan). Data were collected by a computer interface established using HP-Vee Pro software. The measurements were carried out at different temperatures in a temperature controlled furnace. The measured capacitance and conductance were converted to the dielectric constant and conductivity.

III. RESULTS

A powder XRD pattern of the sintered $KNbO_3$ ceramics is shown in Fig. 1. The vertical lines represent the peak positions of the International Centre for Diffraction Data (ICDD: 32-0822) and the variations in the heights represent their respective intensity. It is seen from Fig. 1 that the recorded pattern matches very well with ICDD data, which indicates that the sintered sample exhibits a single phase. The Bragg refections are indexed to the orthorhombic crystal system.

A. Dielectric relaxation

The temperature dependence of the real part of the dielectric permittivity at a few representative frequencies is shown in Fig. 2(a). The data shown in Figs. 2(a) and 2(b) are taken during the cooling process of the thermal cycle. The upward arrows in Fig. 2(a) at two temperatures denote the well-known dielectric anomalies of potassium niobate. The first one at 213 °C corresponding to the ferroelectric–orthorhombic to ferroelectric–tetragonal phase transition. And, the second one at 420 °C is the ferroelectric–tetragonal to paraelectric–cubic phase transition.[2] The Curie temperature shifted to low temperature by 15 °C to that of single crystal ($T_C = 435$ °C).[2] This is ascribed to hysteresis and a possible off stoichiometry of the polycrystalline samples.

It is seen from Fig. 2(a) that at any given temperature other than the anomaly regions, the dielectric constant decreases with an increase in frequency and the dependence of dielectric constant with frequency increasingly varies with temperature. Such behavior is not observed in isostructural $BaTiO_3$ ceramics. Also, a hump observed in the temperature range of 150 to 200 °C [the encircled part of the curve in Fig. 2(a)] shows frequency dependency. The corresponding feature is marked by a circle in the tangent loss curves [see Fig.
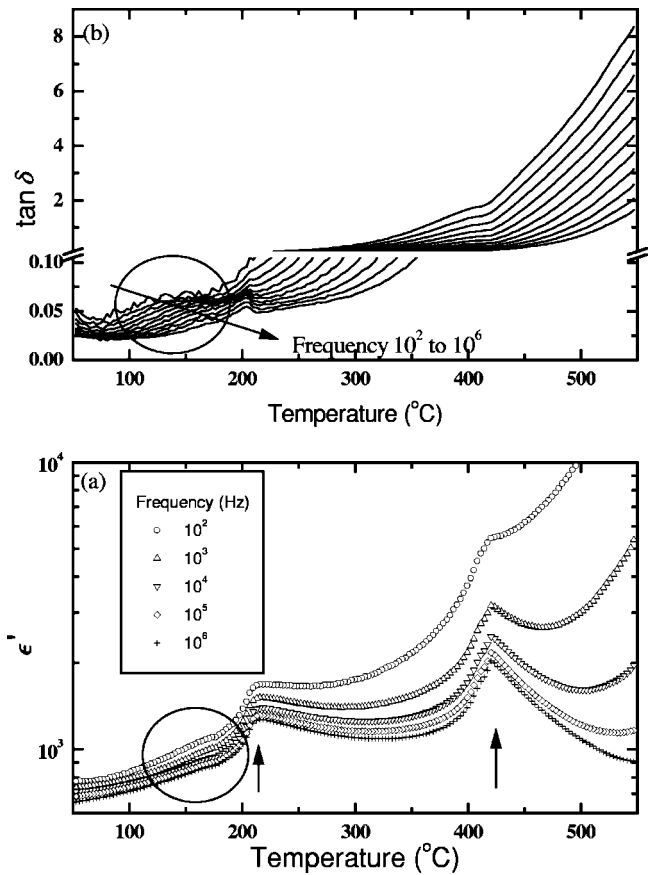

FIG. 2. (a) Real part of the dielectric permittivity and (b) the tangent loss curves as a function of temperature for different frequencies.

2(b)] and the variation of the frequency is indicated by an arrow. The peak position temperatures of loss peaks between 100 and 200 °C increase with an increase in frequency and this indicates a frequency dispersion. This observation is related to the dielectric relaxation.

To understand the dielectric relaxation, the semiempirical complex Cole–Cole equation was used to analyze the data[8]

$$\epsilon^* = \epsilon' - i\epsilon'' = \epsilon_\infty + (\epsilon_s - \epsilon_\infty)/[1 + (i\omega\tau)^\beta], \quad (1)$$

where ϵ_s is the static dielectric constant, ϵ_∞ is the dielectric constant at high frequency, ω is angular frequency, τ is mean relaxation time, and $\beta = 1 - \alpha$, where α is the angle made with the axis of the real part of dielectric permittivity to the center of the semicircular arc.

Figure 3 shows the Cole–Cole plot with a fitting to experimental data at four different temperatures using Eq. (1). The fitting was performed with a least-square minimization method.

The real and imaginary parts of the dielectric permittivity are written as[9,10]

$$\epsilon' = \epsilon_\infty + (\Delta\epsilon'/2)\{1 - \sinh(\beta z)/[\cosh(\beta z)$$
$$+ \cos(\beta\pi/2)]\}, \quad (2)$$

$$\epsilon'' = (\Delta\epsilon'/2)\sin(\beta\pi/2)/[\cosh(\beta z) + \cos(\beta\pi/2)], \quad (3)$$

where $z = \ln(\omega\tau)$ and $\Delta\epsilon' = \epsilon_s - \epsilon_\infty$.

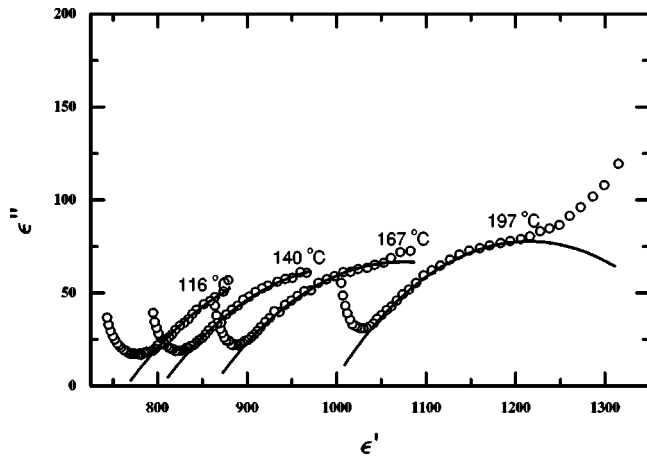Figure 4 shows the real and imaginary parts of dielectric

FIG. 3. Cole–Cole plot at different temperatures. The solid semicircular arcs through the data are obtained by fitting the data to the Cole–Cole equation.

permittivity as a function of frequency and the solid lines passing through the data points are calculated using Eqs. (2) and (3) which utilize the parameters obtained from the Cole–Cole fitting. It is seen from the graph in Fig. 4 that fitting matches the data points in the relaxation region marked by upward arrows.

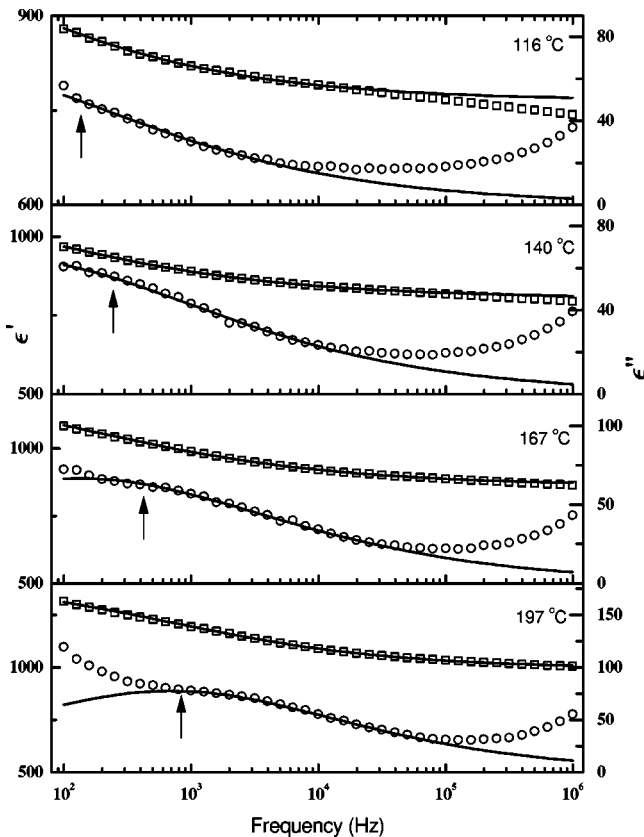The thermally driven relaxation process in the tempera-

FIG. 4. Real (□) and imaginary (○) parts of the dielectric constant plotted as a function of frequency at four temperatures. Solid lines are calculated using Eqs. (2) and (3). The upward arrows indicate loss peaks at different temperatures.
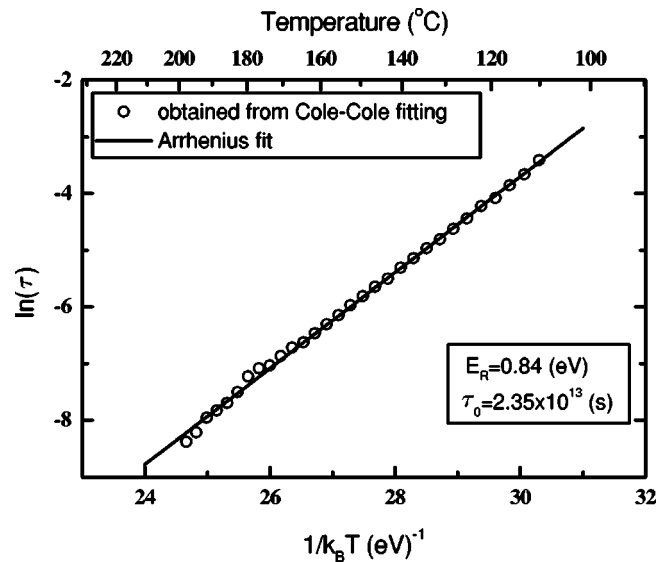

FIG. 5. Arrhenius plot for the relaxation time in the temperatures between 100 to 200 °C. The solid line through the data is a linear fit to Eq. (4).

ture range of 100 to 200 °C is described by the Arrhenius equation of the following form:

$$\tau = \tau_0 \exp(E_R / k_B T). \tag{4}$$

Figure 5 shows the Arrhenius plot wherein the data points are obtained from Cole–Cole fitting and the solid line passing through data points is a linear fit to Eq. (4). The activation energy, E_R, of the relaxation process is calculated to be 0.84 eV and the preexponential factor, τ_0, is 2.35×10^{13} s, which is of the order of the lattice vibrational phonon frequency.

B. ac conductivity

The frequency dependent conductivity of inorganic glasses, polymers, doped semiconductors, and ionic conductors exhibits a universality and their behavior is scaled to master curve (i.e., conductivity data follow the time–temperature superposition).[11–17] The frequency dependent conductivity is well described by the known augmented Jonscher relation as

$$\sigma'(\omega) = \sigma_{dc} \left[1 + \left(\frac{\omega}{\omega_H} \right)^n \right] + A\omega, \tag{5}$$

where σ_{dc} is the dc conductivity, ω_H is onset frequency of the ac conductivity/mean frequency of the hopping process, n is the exponent vary between 0.5 to 1, and A is weakly temperature dependent term of the form $\exp(T/T_0)$. Two terms of Eq. (5) are denoted as, namely, universal dielectric response (UDR), in general, universal dynamic response, and nearly constant loss (NCL), respectively. These two additive terms correspond to different processes happening in the material. The power-law frequency dependent UDR term originates from the hopping of the carriers with interactions of the inherent defects or disorder in the material. Whereas, the linear frequency dependent NCL term is modeled to originate from rocking motions in a asymmetric double well potential[17] and electrical loss occurring during the time re-
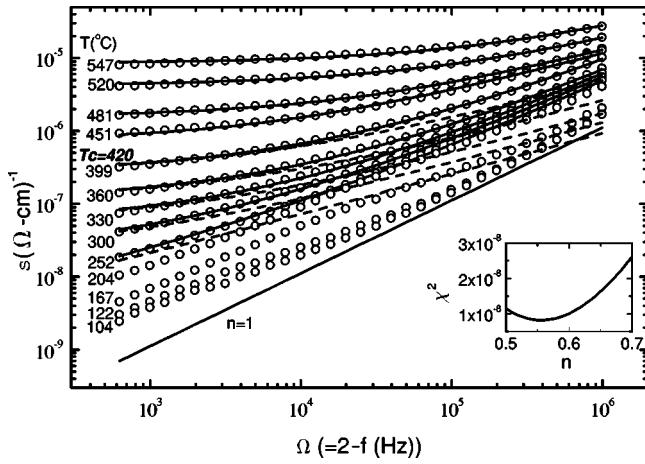
FIG. 6. The typical frequency dependent conductivity data at a few temperatures are plotted. The solid lines through the data points are nonlinear least-squares fit to the Eq. (5). The dashed lines are calculated using the first term of Eq. (5), where the parameters are obtained from fitting done with the both the terms of Eq. (5). The inplot shows the least-squares minimum when n varied between 0.5 to 0.7. Solid line marked with $n = 1$ represent the slope with unity.

FIG. 7. Arrhenius plot of the dc conductivity ($\bigcirc$) and hopping frequency ($\square$). The sold lines are the respective linear fits to the Eqs. (6) and (7).

gime while the ions are confined to the potential energy minimum.[18] UDR and NCL terms are further categorized to occur in the high-temperature/low-frequency and the low-temperature/high-frequency regimes, respectively.

To understand the dielectric constant variation as a function of frequency at a given temperature, frequency dependent conductivity measurements were performed. The ac-conductivity data of potassium niobate with nonlinear least-square fitting to Eq. (5) with a statistical weighting is shown in Fig. 6. The ac-conductivity data at the temperatures of 547, 520, 481, and 451 °C, above the Curie temperature, are fitted only with UDR term. Also, in the fitting process, exponent in the UDR term is fixed at 0.56, i.e., n is kept independent of temperature. The exponent value is reported to be 0.6 for many of the materials.[17] The value of exponent as 0.56 is justified from the minimum of χ^2 values while varying n from 0.5 to 0.7. The resultant χ^2 is shown in the inset of Fig. 6, which shows a minimum at 0.56. Data below the Curie temperature are fitted with both the terms of the augmented Jonscher equation since, at high frequencies, the variation of the conductivity is close to unity (solid straight line in Fig. 6 marked with $n = 1$ represents the slope of the log–log plot to be unity) and the imaginary part of permittivity is nearly constant $\epsilon''(\omega) = \sigma'(\omega)/\epsilon_0\omega$. A marked difference in the shape of conductivity curves below the Curie temperature envisages the need of NCL term.[6] The dashed lines in Fig. 6 are generated by keeping the NCL term as 0 while the other parameters are kept constant, which explicitly shows the NCL part of ac conductivity. The data below 200 °C is not fitted due to the convolution of the relaxation features with the conductivity data.

The temperature variation of the dc conductivity, σ_{dc}, and the hopping frequency, ω_H, are described by the Arrhenius equation:

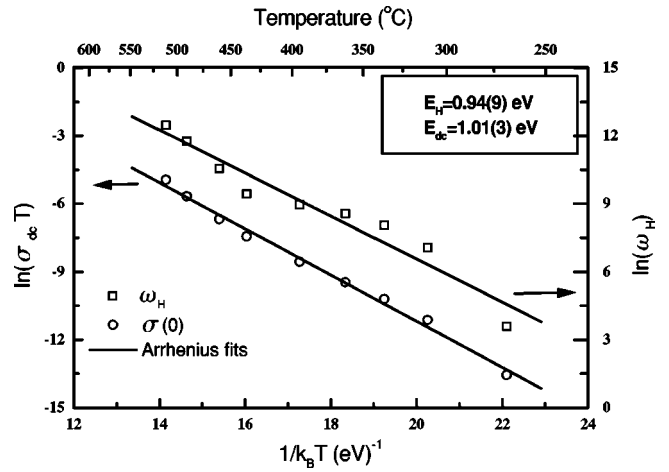$$\sigma_{dc}T = \sigma_0 \exp(-E_{dc}/k_BT), \tag{6}$$

$$\omega_H = \omega_0 \exp(-E_H/k_BT), \tag{7}$$

where E_{dc} and E_H are the activation energies of the dc conductivity and hopping frequency of the carriers, respectively.

Figure 7 shows the Arrhenius plot of the dc conductivity and the hopping frequency, respectively, obtained from fitting the data to the augmented Jonscher relation and the solid line is a linear fit to the Eqs. (6) and (7). The calculated activation energies of the dc conductivity and the hopping frequency are 1.01(3) and 0.94(9) eV, respectively. The measured activation energy of the dc conductivity matches that of the reported value, 1.02 eV.[6]

IV. DISCUSSION

The complex dielectric susceptibility function for the decay of polarization in the Debye model is $\chi(0)[1/(1 + \omega^2\tau^2) - i\omega\tau/(1 + \omega^2\tau^2)]$. The function has a peak in the imaginary part of permittivity or tangent loss ($\tan\delta = \epsilon''/\epsilon'$) curve with a single relaxation time when $\omega\tau = 1$, which is associated with the dielectric relaxation. For most solids, different from that liquids, the relaxation process exhibits a distribution of relaxation times.[19]

The origin of the dielectric relaxation due to the motion of the domain walls, long-range disorders, interfacial polarization, and thermal motion of ions to different sites, etc., is reported in literature. Relaxation modes in $Ba(Ti_xZr_{1-x})O_3$ were attributed to long-range disorder and the authors also pointed out that the relaxation process was not related to the grain-boundary effects from similar observations in both the polycrystalline and single crystals.[20] Pyrochlore $Cd_2Nb_2O_7$ was also shown to exhibit dielectric relaxation due to the motion of the domain walls analogous with triglycine sulphate behavior.[9]

In materials like doped (La, Bi, and Fe)–$SrTiO_3$,[10,21,22] $BaTiO_3$,[23] and Ca-doped $KTa_{1-x}Nb_xO_3$,[24] the dielectric relaxation is associated with defect-induced relaxations. For instance, a recent report on Bi–$SrTiO_3$ revealed that the oxygen-vacancy-related dipoles cause dielectric relaxation

rather than the interfacial polarization or the hopping of Ti ions to more than one of the off-center available sites due to the distortion of oxygen octahedra(TiO_6).

Presently, a frequency dispersion of the loss peak is observed in the temperature range of 100 to 200 °C on undoped $KNbO_3$ [see Fig. 2(b)] and the corresponding activation energy is estimated to be 0.84 eV (see Fig. 5). The activation energy is relatively higher than that of the materials reported in literature.[10,21–24] Possible origins of dielectric relaxation are scrutinized next. The present observation is not associated with a probable pretransitional, orthorhombic–ferroelectric to tetragonal–ferroelectric phase transition, fluctuations triggered by a possible cubic anharmonicity due to the broad width ($\sim$100 °C) of the loss peaks and also the observation is reasonably far from the transition temperature. Dielectric relaxations originating from long-range positional order/disorder of cations and vacancies are not considered due to the absence of any satellite peaks in XRD patterns (see Fig. 1). Lian et al.[25] reported that domain-wall motions exhibit active behavior in a small temperature range across the orthorhombic to tetragonal phase transition of potassium niobate. The temperature range is about 10 °C in the orthorhombic phase and 15 °C in the tetragonal phase. But, the dielectric relaxation is presently observed over the broad temperature range of $\sim$100 °C and has single activation energy. This precludes domain-wall motions to be the reason for dielectric relaxation. Maxwell–Wagner or interfacial polarizations arising from inhomogenious microstructures are usually considered in materials with extremely high dielectric permittivity.[26] In the present observation, the dielectric permittivity of potassium niobate is around 1000 at the temperature and frequency of 150 °C and 10^2 Hz, respectively. This is an order of magnitude smaller, which suggests that interfacial polarizations are probably not involved in the dielectric relaxation. In view of these considerations, the dielectric relaxation is associated with the decay of polarization in the defect related dipoles.

Potassium oxide volatility commonly causes difficulty in the growth of single crystals and preparation of ceramics. A revised phase diagram and the evaporation of potassium oxide were clearly established by Flückiger and Arend[27] from the thermal analysis of the KN crystals heat treated at different temperatures (950 to 1050 °C) and times. Also, it has been reported in literature that excess potassium oxide was used in the precursor materials during the $KNbO_3$ single crystal growth[28] and thin-film preparation.[29,30] The potassium oxide evaporation results in a nonstoichiometry and the defect structure can be written as

$$K_K \rightarrow K + V'_K + h^{\cdot}, \tag{8}$$

$$O_O \rightarrow 1/2(O_2) + V_O^{\cdot\cdot} + 2e', \tag{9}$$
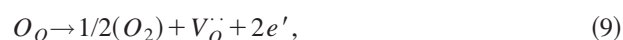
where V'_K is a potassium vacancy with a negative charge and $V_O^{\cdot\cdot}$ is an oxygen vacancy with two positive charges.

Defect-related dipoles are active in the externally applied fields. An analysis of the ac conductivity has yielded activation energies of dc conductivity and hopping frequency to be 1.01(3) and 0.94(9) eV, respectively. It is to be noted that the activation energy of the dielectric relaxation is close to that of dc conductivity (see Fig. 7). This suggests the involvement of the mobile charge carriers in the dielectric relaxation process.

The prime origin of the ac conductivity of the ionic materials[16] and oxides[17,31] is due to the hopping of the carriers. In potassium niobate, similar values (see Fig. 6) of the activation energies, E_{dc} and E_H, indicate that the frequency dependent conductivity originates from hopping of the carriers.

Hopping carrier is inferred from the analogy with literature on ferroelectric perovskites. Oxide ion conduction in Mg substituted $KNbO_3$ is established from the dependence of conductivity on oxygen partial pressure. Also, the slope change in the Arrhenius plot corresponding to the extrinsic and intrinsic regions occurs around 550 °C in the 10 mole present Mg-substituted KN.[32] La-doped $Na_{0.5}Bi_{0.5}TiO_3$ exhibits oxygen vacancy conduction with an activation energy around 1 eV and the two regions are separated at the temperature of 700 °C.[33] The dominant charge carrier in the $BaTiO_3$ and $Pb(Zr_{1-x}Ti_x)O_3$ is reported to be oxygen vacancies.[34] Importantly, an experimental estimate of the activation energy for oxygen vacancy migration in potassium niobate is reported to be around 1 eV.[35] Based on the aforementioned literature on ferroelectric perovskites and in consideration of the ionic radius (K^+:1.64, Na^+:1.39, Ba^{2+}:1.61, and Pb^{2+}:1.49 Å, where CN is 12) and activation energies, the most probable hopping carrier is presumed to be oxygen vacancy. Also, it is reasonable to assume from literature on isostructural materials that the temperature range of the present investigation is pertinent to the extrinsic region.

The point defect concentration of the potassium vacancy, V'_K, would be double that of an oxygen vacancy, $V_O^{\cdot\cdot}$. It is equally possible that potassium migration can also contribute to the ionic conduction process. Computational simulations of the ionic transport in perovskite oxides indicate that the activation energy for oxygen vacancy migration is around 1 eV, for the A-site cation transport is around 4 eV, and for the B-site cation migration is around 14 eV.[36] The observed activation energy for the dc conductivity matches with the oxygen vacancy migration. Hence, cation migration is less likely to happen in the ionic conduction process.

The spontaneous polarization originating from the ionic or displacement dipoles is known to be the off center displacement of Nb^{5+} ions from the anionic charge center of the oxygen octahedron. The presence of oxygen vacancies in the off-stoichiometric sample would distort the actual ionic dipoles due to Nb^{5+} ions. The decay of polarizations due to distorted ionic dipoles may also be the cause for the presently observed dielectric relaxation. Kotomin et al.[37] reported that the activation energy for the Nb^{5+} ion relaxation to the oxygen vacancies is 3.6 eV from ab initio and semi-empirical calculations. Due to the difference in the activation energies, relaxations involving thermal motions Nb ions are not a probable process. Hence, it is reiterated that the low-frequency relaxations observed from the present study is the decay of polarization in the oxygen defect-related dipoles due to their hopping conduction.

Potassium niobate is one of the candidate materials for

environmental friendly piezoelectric ceramics. Poling of ceramics is necessary for the piezoelectric measurements and applications. Wada *et al.*[38] reported that poling of the KN crystals was attained when performed at temperatures higher than 100 °C. Also, poling at those temperatures is commonly practiced in piezoelectric ceramics. But, KN ceramics show that the dielectric relaxation would hinder the poling process carried out at temperatures above 100 °C. For applications of potassium niobate ceramics, it is desired that samples show no dielectric relaxations. This creates a scope for the further work on KN ceramics. Further understanding may be obtained from the dielectric measurements in a range of nonstoichiometric samples produced by changing the molar ratio of the reactants.

V. CONCLUSION

The activation energies of the thermally driven low-frequency dielectric relaxation and conductivity processes are obtained. The mechanism of the low-frequency dielectric relaxation is proposed due to relaxations in oxygen vacancy-related dipoles. And, the frequency dependent conductivity is due to the oxygen vacancy hopping conduction. The inadvertent potassium oxide evaporation during the synthesis process leads to the nonstoichiometric potassium niobate, which provides the channels for hopping conduction.

ACKNOWLEDGMENTS

[1] D. Xue and S. Zhang, Chem. Phys. Lett. **291**, 401 (1998).

[2] B. F. Jona and G. Shirane, *Ferroelectric Crystals* (Dover, New York, 1993), p. 221.

[3] H. Nagata and T. Takenaka, Jpn. J. Appl. Phys., Part 1 **36**, 6055 (1997); **37**, 5311 (1998).

[4] P. Dubernet and J. Ravez, Ferroelectrics **211**, 51 (1998).

[5] C. Prieto, L. Arizmendi, J. A. Gonzalo, F. Jaque, and F. A. Lopez, Phys. Rev. B **31**, 5483 (1985).

[6] C. Lee, S. Lee, C. Sul, and S. Bae, Physica B **239**, 316 (1997).

[7] U. Flückiger, H. Arend, and H. R. Oswald, Ceram. Bull. **56**, 575 (1977).

[8] K. S. Cole and R. H. Cole, J. Chem. Phys. **9**, 341 (1941).

[9] C. Ang, R. Guo, A. S. Bhalla, and L. E. Cross, J. Appl. Phys. **87**, 7452 (2000).

[10] C. Ang, Z. Yu, and L. E. Cross, Phys. Rev. B **62**, 228 (2000).

[11] J. C. Dyre and T. B. Schrøder, Rev. Mod. Phys. **72**, 873 (2000).

[12] B. Roling, A. Happe, K. Funke, and M. D. Ingram, Phys. Rev. Lett. **78**, 2160 (1997).

[13] D. L. Sidebottom, Phys. Rev. Lett. **82**, 3653 (1999).

[14] A. S. Nowick, A. V. Vaysleyb, and I. Kuskovsky, Phys. Rev. B **58**, 8398 (1998).

[15] B. Roling, C. Martiny, and C. Murugavel, Phys. Rev. Lett. **87**, 085901 (2001).

[16] A. Rivera, C. León, J. Sanz, J. Santamaria, C. T. Moyniham, and K. L. Ngai, Phys. Rev. B **65**, 224302 (2002).

[17] A. S. Nowick and B. S. Lim, Phys. Rev. B **63**, 184115 (2001).

[18] C. León, A. Rivera, A. Várez, J. Sanz, J. Santamaria, and K. L. Ngai, Phys. Rev. Lett. **86**, 1279 (2001).

[19] K. L. Ngai, Comments Solid State Phys. **9**, 127 (1979).

[20] Z. Yu, R. Guo, and A. S. Bhalla, J. Appl. Phys. **88**, 410 (2000).

[21] T. Y. Tien and L. E. Cross, Jpn. J. Appl. Phys., Part 1 **6**, 459 (1967); E. Iguchi and K. J. Lee, J. Mater. Sci. **28**, 5809 (1993).

[22] C. Ang, Z. Yu, Z. Jing, P. Lunkenheimer, and A. Loidl, Phys. Rev. B **61**, 3922 (2000).

[23] R. Stumpe, D. Wagner, and D. Bauerle, Phys. Status Solidi A **75**, 143 (1983).

[24] G. A. Samara and L. A. Boatner, Phys. Rev. B **61**, 3889 (2000).

[25] Li Lian, T. C. Chong, H. Kumagai, M. Hirano, L. Taijing, and S. C. Ng, J. Appl. Phys. **80**, 376 (1996).

[26] I. Burn and S. Neirman, J. Mater. Sci. **17**, 3510 (1982).

[27] U. Flückiger and H. Arend, J. Cryst. Growth **43**, 406 (1978).

[28] C. Y. Beh, T. C. Chong, H. Kumagai, and M. Hirano, J. Cryst. Growth **171**, 501 (1997).

[29] A. Onoe, A. Yoshida, and K. Chikuma, Appl. Phys. Lett. **69**, 167 (1996).

[30] K. Kakimoto, S. Ito, I. Masuda, and H. Ohsato, Jpn. J. Appl. Phys., Part 1 **41**, 6908 (2002).

[31] S. Saha and T. P. Sinha, Phys. Rev. B **65**, 134103 (2002).

[32] L. Li, G. Li, R. L. Smith, Jr., and Inomata, Appl. Phys. Lett. **81**, 2899 (2002).

[33] J. Y. Yi, J.-K. Lee, and K.-S. Hong, J. Am. Chem. Soc. **85**, 3004 (2002).

[34] M. V. Raymond and D. M. Smyth, J. Phys. Chem. Solids **57**, 1507 (1996).

[35] D. M. Smyth, Ferroelectrics **151**, 115 (1994).

[36] M. S. Islam, J. Mater. Chem. **10**, 1027 (2000).

[37] E. A. Kotomin, N. E. Christensen, R. I. Eglitis, and G. Borstel, Comput. Mater. Sci. **10**, 339 (1998).

[38] S. Wada, A. Seike, and T. Tsurumi, Jpn. J. Appl. Phys., Part 1 **40**, 5690 (2001).